Table VII. Recalculated Magnetic Data for the Red Iron Compounds

compd	T, K	$10^6 \times \chi_m^{cor}$, emu mol^{-1}	μ_{eff}, μ_B
$[Fe(phen)_3]_2[Fe(ox)_3](ox)_{1/2}\cdot 14H_2O$	399.4	5863	4.33
	294.2	6847	4.01
	189.5	9568	3.91
	76.8	22258	3.70
$[Fe(phen)_3]_2[Fe(mal)_3](mal)_{1/2}\cdot 20H_2O$	359.7	5528	3.99
	293.3	6329	3.85
	190.2	9157	3.73
	75.7	22048	3.65
$[Fe(4,7\text{-}(CH_3)_2\text{-}phen)_3]_2[Fe(ox)_3]\text{-}(ox)_{1/2}\cdot 14H_2O$	293	7452	4.18
	195	10308	4.01
	77	23106	3.77
$[Fe(4,7\text{-}(CH_3)_2\text{-}phen)_3]_2[Fe(mal)_3]\text{-}(mal)_{1/2}\cdot 20H_2O$	293	7513	4.20
	195	10732	4.09
	77	25267	3.94
$[Fe(bpy)_3]_2[Fe(ox)_3](ox)_{1/2}\cdot 8H_2O$	293	7440	4.18
	195	10380	4.02
	77	23671	3.98
$[Fe(bpy)_3]_2[Fe(mal)_3](mal)_{1/2}\cdot 8H_2O$	293	6566	3.92
	195	9599	3.87
	77	23372	3.79

The results of magnetic measurements reported previously for solid samples of the red complexes have been converted to the new molecular weights. A number of characteristic values, always referring to a single Fe atom, are listed in Table VII. It is evident that the values of μ_{eff} are consistent with the proposed stoichiometry of the complexes. Let us assume that a high-spin iron(III) complex such as $[Fe(ox)_3]^{3-}$ is characterized by $\mu_{eff} = 5.90\ \mu_B$ and a low-spin iron(II) complex such as $[Fe(phen)_3]^{2+}$, by $\mu_{eff} = 0.60\ \mu_B$. For a Fe(II):Fe(III) = 2:1 complex, we obtain then $\mu_{eff} = 3.44\ \mu_B$, a value somewhat lower than the measured values. Again, the difference is not significant and may be caused, among others, by a difference in hydration of the complexes.

The nature of the red iron compounds has thus been clarified by the present results, and these results will have consequences for all those studies where the formation of an $S = 1$ ground state of iron(II) has been inferred on the basis of magnetic and similar nonspecific data. As typical examples we refer to a number of bis(thiocyanato)bis(substituted 1,10-phenanthroline)iron complexes,[12] to bis((cyano-*C*)trihydroborato)bis(1,10-phenanthroline)iron,[13] and to the thermolysis of (oxalato)bis(1,10-phenanthroline)iron(III) hydrogen oxalate.[14] Additional complexes for which a reinvestigation is desirable may be found from tabulated results of magnetic measurements.[15]

Acknowledgment. The authors appreciate financial support by the Stiftung Volkswagenwerk.

Registry No. **1**, 78591-89-6; **2**, 78591-90-9; **3**, 78591-91-0; **4**, 78591-92-1; **5**, 78591-55-6; **6**, 78591-93-2; $Fe(phen)_2ox$, 14783-55-2; $Fe(phen)_2mal$, 14592-32-6; $Fe(4,7\text{-}(CH_3)_2\text{-}phen)_2ox$, 21515-94-6; $Fe(4,7\text{-}(CH_3)_2\text{-}phen)_2mal$, 14767-27-2; $Fe(bpy)_2ox$, 21515-92-4; $Fe(bpy)_2mal$, 14881-83-5; $[Fe(phen)_3](ClO_4)_2$, 14586-54-0; $[Fe(4,7\text{-}(CH_3)_2\text{-}phen)_3](ClO_4)_2$, 15712-32-0; $[Fe(bpy)_3](ClO_4)_2$, 15388-48-4; $[Fe(phen)_3]Cl_2$, 14978-15-5; $[Fe(4,7\text{-}(CH_3)_2\text{-}phen)_3]Cl_2$, 78591-94-3; $[Fe(bpy)_3]Cl_2$, 14751-83-8; $K_3[Fe(ox)_3]$, 14883-34-2; $Na_3[Fe(ox)_3]$, 5936-14-1; $X_3[Fe(mal)_3]$, 50770-87-1.

(12) Cunningham, A. J.; Ferguson, J. E.; Powell, H. K. J.; Sinn, E.; Wong, H. *J. Chem. Soc. Dalton Trans.* **1972**, 2155.
(13) Purcell, K. F.; Yeh, S. M.; Eck, J. S. *Inorg. Chem.* **1977**, *16*, 1708.
(14) Thomas, P.; Benedix, M.; Rehorek, D.; Hennig, H. *Z. Chem.* **1978**, *18*, 264.
(15) König, E.; König, G. "Magnetic Properties of Coordination and Organometallic Transition Metal Compounds". Landolt-Börnstein, New Series; Springer: Berlin, New York; 1976, Vol. II/8; 1979, Vol. II/10; 1981, Vol. II/11.

Contribution from the Department of Chemistry, University of Windsor, Windsor, Ontario N9B 3P4, Canada

Proton NMR Study of the High-Spin–Low-Spin Transition in $Fe(phen)_2(NCS)_2$ and $Fe(pic)_3Cl_2\cdot$(EtOH or MeOH)

P. SAMBASIVA RAO, PRABUDDHA GANGULI, and BRUCE R. McGARVEY*

Received December 19, 1980

The proton NMR spectra of spin-crossover complexes $[Fe^{II}(phen)_2(NCS)_2]$ (phen = 1,10-phenanthroline) and $[Fe^{II}(pic)_3]Cl_2\cdot X$ (X = CH_3OH or C_2H_5OH) (pic = 2-(aminomethyl)pyridine) and their Zn(II) analogues have been determined for temperatures that span the crossover region. The line widths of all Fe(II) complexes are constant in the diamagnetic temperature region but increase markedly in the spin-transition region. At higher temperatures the line width follows a T^{-1} dependence. Second-moment measurements in the diamagnetic region reveal a close contact (~0.18 nm) between hydrogen atoms on neighboring complexes in the case of $Fe(phen)_2(NCS)_2$. The asymmetric broad lines in the paramagnetic region are quantitatively accounted for by using a point-dipole model of the paramagnetic shift. T_1 vs. temperature studies were made for $Fe(phen)_2(NCS)_2$, and the results are shown to be in conflict with predictions of a "cluster" or domain theory for the spin crossover. The results are in complete agreement with an Ising-type theory of the transition, and it is shown that the T_1 measurements readily yield several of the thermodynamic parameters in the theory.

I. Introduction

We recently completed an ESR[1] study of Mn(II) doped into $[Fe^{II}(phen)_2(NCS)_2]$ (phen = 1,10-phenanthroline) and $[Fe^{II}(pic)_3]Cl_2\cdot$EtOH (pic = 2-(aminomethyl)pyridine). These systems undergo a spin transition over a small temperature interval from a diamagnetic ($S = 0$) system at low temperatures to a paramagnetic ($S = 2$) system at higher temperatures. Our ESR studies confirmed that no phase transition of the crystal lattice accompanies this spin transition. We undertook a proton NMR study of these systems to see if additional information on the mechanism of this spin transition could be gained from this physical technique.

The spin crossover is very abrupt or discontinuous for $Fe(phen)_2(NCS)_2$, but the sharpness and even the crossover temperature vary with preparation. In many instances there is found a residual paramagnetism at low temperatures

(1) Rao, P. S.; Reuveni, A.; McGarvey, B. R.; Ganguli, P.; Gütlich, P. *Inorg. Chem.* **1981**, *20*, 204.

0020-1669/81/1320-3682$01.25/0

amounting to 5–15% of the total Fe(II) ions. The transition has been studied by using Mössbauer[2-4] spectroscopy, magnetic susceptibility,[2,3,5,6] far-infrared spectroscopy,[7-9] heat capacity measurements,[9] and XPES X-ray methods.[10] The only NMR study was by Dezsi et al.,[3] who reported on the line width variation with temperature but gave no interpretation or explanation of their results.

The transition in $Fe(pic)_3Cl_2$·EtOH is more gradual, taking place over a 50 °C interval. It was first reported by Renovitch and Baker,[11] who studied it by magnetic susceptibility and Mössbauer spectroscopy. Further studies by Mössbauer spectroscopy[12] showed that the replacement of C_2H_5OH by CH_3OH or H_2O had a marked effect on the nature of the spin transition. Zn(II) dilution studies[13,14] on the compound showed that the transition still took place, but T_c (the temperature at which the system is 50% high spin) decreased with increasing concentration of Zn(II).

Various theories have been put forward to account for the nature of the spin transition in these and other systems. König and Kremer[15] tried to fit the magnetic data to a crystal field model in which the lowest state of Fe(II) is $^1A_1$ with the excited state $^5T_2$ being close in energy to the ground state. They found that their model would fit the data only if the average energy separation between the $^5T_2$ and $^1A_1$ states varied dramatically with temperature in the transition region. Zimmermann and König[16] have shown that the experimental data can be fit to a model in which an interaction term is introduced such that the energy of the $^1A_1$ and $^5T_2$ states of a given ion depends on the spin state of neighboring ions. It was assumed that this interaction term resulted from a change in the ligand field at a given ion caused by a change in the size of a neighboring complex when it changed from low to high spin. It is known that the high-spin iron complex has weaker and longer Fe–N bonds. The ESR of Mn(II) in these systems[1] casts doubt on this explanation for the origin of the interaction term because no change in the crystal field of Mn(II) could be observed when the neighboring Fe(II) ions changed from low to high spin.

Sorai and Seki[9] proposed a cluster or domain theory, which was extended by Gütlich et al.[17] In this model they proposed that the transformation took place in domains having n complexes and that within the domain all iron ions have the same spin. Fitting the heat capacity data to the theory, they found $n = 95$ for $Fe(phen)_2(NCS)_2$. Although no cooperative interaction term appears in the theory such as proposed by Zimmermann and König,[16] it is implicit in their assumption of stable high-spin domains. To date no experimental data can select between the two theories described above.

The present work was undertaken in the hope that a study of the temperature dependence of the proton NMR line shapes and relaxation times would help to distinguish between present theories of the spin transition. It was also hoped that something could be learned about the nature and origin of the cooperative interaction between neighboring Fe(II) ions. Both hopes were fulfilled.

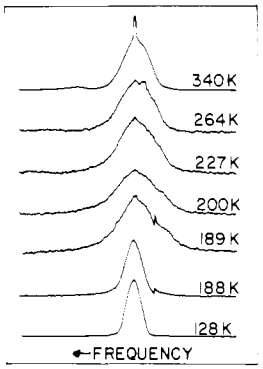

Figure 1. Typical NMR spectra of $Fe(phen)_2(NCS)_2$ (ext). The frequency increases from right to left in these plots.

II. Experimental Section

A. Chemical Preparation. The preparation of $Fe(phen)_2(NCS)_2$ (precipitated (ppt)) and $Fe(pic)_3Cl_2$·EtOH was given earlier.[1] $Fe(phen)_2(NCS)_2$ (extracted (ext)) was prepared with use of the method of Madeja et al.,[18] in which $[Fe(phen)_3](NCS)_2$ is refluxed with acetone or other organic solvents to remove one molecule of 1,10-phenanthroline.

$Fe(pic)_3Cl_2$·MeOH was prepared by adding 2-(aminomethyl)-pyridine dropwise to a well-stirred solution of $FeCl_2$·$2H_2O$ (0.004 mol) in methanol. The precipitated complex was filtered off and dried over P_2O_5 in vacuum for several hours.

All preparations were done in a dry-nitrogen atmosphere. The corresponding Zn complexes were prepared in the same manner with use of stoichiometric amounts of $ZnCl_2$ in place of $FeCl_2$. The purity of the samples were confirmed by elemental analysis and IR spectra.

B. NMR Spectra. The samples were sealed under vacuum in 10 mm diameter tubes for NMR measurements. The spectra were taken at 90.02 MHz on a Bruker CXP-100 high-power FT spectrometer. The transmitting–receiving coil was detuned slightly by introducing additional resistance in series with the coil to give a linear response over a 1-MHz bandwidth. B_1 was about 1.2–1.4 mT and 10° pulses were used to get best representation of the broad lines observed. Both quadrature and nonquadrature detection were used with no observed difference in line shapes.

T_1 measurements were made by using a 180° pulse followed by a detection pulse. In these measurements quadrature detection was used with the carrier frequency placed in the center of the resonance. The time dependence of the center portion of the broad line was followed and fitted to a three-parameter curve by least squares to obtain T_1 values.

The temperature was controlled and measured by a Bruker BVT-1000 variable-temperature accessory. Since this accessory measures the temperature by a Cu–constantan thermocouple placed ahead of the sample in the N_2 gas flow, we prepared calibration curves by measuring the temperature inside an identical sample and tube with a second thermocouple. In general we found the difference to be less than 5 °C at the lowest temperatures studied.

III. Results

A. Line Widths vs. Temperature. 1. $Fe(phen)_2(NCS)_2$. Two samples prepared in different ways were examined. $Fe(phen)_2(NCS)_2$(ppt) had been shown earlier[1,17] by Mössbauer spectroscopy to have ~12% paramagnetic iron at all temperatures below the transition temperature. The spin transition was not discontinuous but took place in a 10 °C interval. The second preparation, $Fe(phen)_2(NCS)_2$(ext), showed[4] no residual paramagnetic iron at low temperatures and a nearly discontinuous transition at about 185 K. This variability with the nature of the preparation and even with

(2) König, E.; Madeja, K. *Inorg. Chem.* **1967**, *6*, 48.
(3) Dezsi, F.; Molnar, B.; Tarnoczi, T.; Tompa, K. *J. Inorg. Nucl. Chem.* **1967**, *29*, 2486.
(4) Ganguli, P.; Gütlich, P. *J. Phys., Colloq. (Orsay, Fr.)* **1980**, *C-1*, 313.
(5) Baker, W. A., Jr.; Bobonick, H. M. *Inorg. Chem.* **1964**, *3*, 1184.
(6) Casey, A. T.; Isaac, F. *Aust. J. Chem.* **1967**, *20*, 2765.
(7) König, E.; Madeja, K. *Spectrochim. Acta, Part A* **1967**, *23A*, 45.
(8) Takenoto, J. H.; Hutchinson, B. *Inorg. Chem.* **1973**, *12*, 705.
(9) Sorai, M.; Seki, S. *J. Phys. Chem. Solids* **1974**, *35*, 555.
(10) Vasudevan, S.; Vasan, H. N.; Rao, C. N. R. *Chem. Phys. Lett.* **1979**, *65*, 444.
(11) Renovitch, G. A.; Baker, W. A., Jr. *J. Am. Chem. Soc.* **1967**, *89*, 6377.
(12) Sorai, M.; Ensling, J.; Hasselbach, K. H.; Gütlich, P. *Chem. Phys.* **1977**, *20*, 197.
(13) Sorai, M.; Ensling, J.; Gütlich, P. *Chem. Phys.* **1976**, *18*, 199.
(14) Gütlich, P.; Link, R.; Steinhäuser, H. G. *Inorg. Chem.* **1978**, *17*, 2509.
(15) König, E.; Kremer, S. *Theor. Chim. Acta* **1971**, *20*, 143.
(16) Zimmermann, R.; König, E. *J. Phys. Chem. Solids*, **1977**, *38*, 779.
(17) Gütlich, P.; Köppen, H.; Link, R.; Steinhäuser, H. G. *J. Chem. Phys.* **1979**, *70*, 3977.
(18) Madeja, K.; Wilke, W.; Schmidt, S. *Z. Anorg. Allg. Chem.* **1966**, *346*, 306.

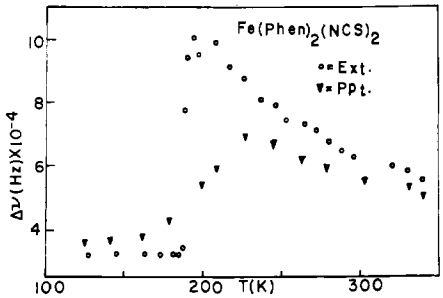

Figure 2. Plot of half-height line widths vs. temperature for two preparations of $Fe(phen)_2(NCS)_2$.

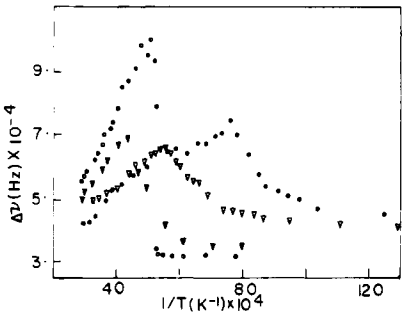

Figure 3. Plot of half-height line widths vs. reciprocal temperature for (○) $Fe(phen)_2(NCS)_2$ (ext), (●) $Fe(pic)_3Cl_2$·EtOH, (▽) $Fe(pic)_3Cl_2$·MeOH, and (▼) $Fe(phen)_2(NCS)_2$ (ppt).

the same preparative method is a problem that has plagued these studies on $Fe(phen)_2(NCS)_2$ from the start.

Representative spectra at different temperatures for $Fe(phen)_2(NCS)_2$(ext) are shown in Figure 1. Below 188 K the line was symmetrical and unchanged while at 189 K it was much broader and unsymmetrical. It was broadest at 200 K, and above that temperature it narrowed slowly with increasing temperature. The sharp lines in the 188 and 189 K curves are due to a strong local FM station whose signal could not always be eliminated. The sharp line at the peak seen in the 340 K curve always appeared near room temperature. Its intensity varied with each preparation and could be decreased somewhat by heating and pumping on the sample. It is most likely due to small amounts of the solvent used in the preparation that could not be removed easily. Such liquid signals were present at higher temperatures in all samples studied in this work. Nothing we tried would remove them entirely.

Defining a line width as the width of the curve at an intensity half the maximum intensity, we obtained the plots of line width vs. temperature shown in Figure 2. Obviously the narrow "liquid lines" observed at the highest temperatures were ignored in determining the maximum intensity of the line. It can be seen that the transition is easily detected in these plots. For reasons that will be developed later, we expected the line widths in the paramagnetic sample to be a linear function of T^{-1}. Therefore, a plot of line width vs. T^{-1} is given in Figure 3 for $Fe(phen)_2(NCS)_2$(ext) to demonstrate this dependence.

Comparison of our line width measurements with those reported by Dezsi et al.[3] shows reasonable agreement below the transition temperature if we assume they measured the peak-to-peak width of the first-derivative curve and that the line shape is approximately Gaussian. Reasonable agreement is also shown at temperatures above the transition if we assume, for reasons to be developed later, that the paramagnetic line width is frequency dependent and correct their widths accordingly.

The different behavior for $Fe(phen)_2(NCS)_2$(ppt) is due to the presence of ~12% paramagnetic iron below the transition, which results in broader lines in this temperature region, and

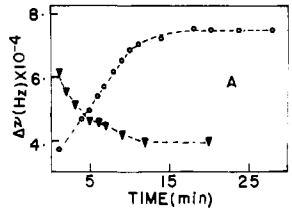

Figure 4. Plot of line width vs. time for the spin transition in $Fe(phen)_2(NCS)_2$ (ext): (○) temperature changed from 188 to 189 K; (▼) temperature changed from 189 to 188 K.

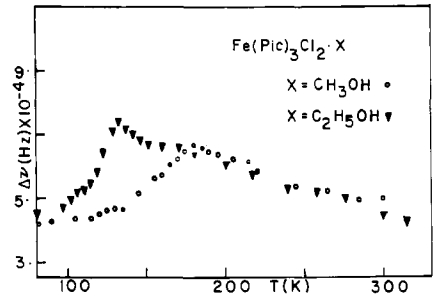

Figure 5. Plot of half-height line widths vs. temperature for two picolylamine complexes.

to the more gradual nature of the transition itself. The line widths approach each other at higher temperatures where both systems are 100% paramagnetic.

When making measurements in the transition region on $Fe(phen)_2(NCS)_2$(ext), we noticed that it took some time before the line width reached an equilibrium value. We, therefore, undertook a crude rate study. We first established equilibrium at 188 K just below the transition and then changed the temperature suddenly to 189 K and measured the line width as a function of time. We also did the reverse experiment in which the temperature was changed from 189 to 188 K. A plot of the results is given in Figure 4. The term "suddenly" is qualitative. We repeated the experiment with a thermocouple inside the sample and found the actual temperature of the sample to change completely in about 1–2 min. The rates measured are much slower than the actual temperature change in the sample. It should be mentioned that good spectra could be observed with 100 pulses having a pulse separation of 0.1 s so that complete spectra were obtained in less than 10 s in these rate studies.

Casey and Isaac[6] reported in a magnetic susceptibility study on $Fe(phen)_2(NCS)_2$ that the high-spin to low-spin conversion in the transition region took 2 h to be complete and followed first-order kinetics. Our measurements show approximate first-order kinetics for the high- to low-spin conversion, but the reaction is over in 15 min. The conversion from low to high spin also takes about 15 min, but the rate approximates more zero-order kinetics. The difference between our results and those of Casey and Isaac[6] may be due to the old problem that the properties of the transition are very dependent on the preparative methods used. Their sample had residual paramagnetism at low temperatures and a lower T_c than our sample. The most that can be said is that we confirm their result that the transformation is slow.

2. $Fe(pic)_3Cl_2$·X. Line widths vs. temperature were measured for X = CH_3OH and C_2H_5OH and are plotted against T in Figure 5 and against T^{-1} in Figure 3. The results are similar to but less dramatic than those found for $Fe(phen)_2(NCS)_2$. The transition is more gradual, as expected, and the line widths are greater in the low-spin region and smaller in the high-spin region than those found in $Fe(phen)_2(NCS)_2$. The larger widths in the low-spin region are due to the presence of more hydrogens at closer distances to each other in these complexes leading to larger dipolar broadening by neighboring

Table I. Second Moments[a] for Low-Spin Forms of Fe(II) Complexes and Their Zn(II) Analogues

complex	M = Fe	M = Zn	theory[b]
$M(phen)_2(NCS)_2$(ext)	2.96 ± 0.25	2.75 ± 0.25	0.56
$M(phen)_2(NCS)_2$(ppt)	9.24 ± 0.25	2.75 ± 0.25	0.56
$M(pic)_3Cl_2$·EtOH	7.02 ± 0.25	5.55 ± 0.25	4.19
$M(pic)_3Cl_2$·MeOH	6.35 ± 0.25	6.17 ± 0.25	4.25

[a] Units are 10^8 Hz^2. [b] Calculated from eq 2.

protons. The broadening in the paramagnetic region is less in the $Fe(pic)_3Cl_2$·X complexes than in the $Fe(phen)_2(NCS)_2$ complexes because the paramagnetic interaction varies as the inverse distance cubed and there are many more protons at larger distances from the Fe(II) ion in the picolylamines than in the phenanthroline complex.

3. Zn Complexes. For control purposes we have prepared the corresponding Zn(II) complexes, which are diamagnetic, and measured their NMR spectra at different temperatures. They all exhibit no change in line width with temperature. The widths of 30 kHz for $Zn(phen)_2(NCS)_2$, 43 kHz for $Zn(pic)_3Cl_2$·MeOH, and 44 kHz for $Zn(pic)_3Cl_2$·EtOH are similar to the widths found for their Fe(II) analogues in the diamagnetic state.

B. Second Moments. We have measured the second moments for the line shape of all iron complexes at low temperatures and of all their Zn(II) analogues. The second moment $\langle \Delta\nu^2 \rangle$ of a line shape function $f(\nu)$ is calculated from

$$\langle \Delta\nu^2 \rangle = \left[\int_0^\infty (\nu - \nu_0)^2 f(\nu)\, d\nu \right] \Big/ \left[\int_0^\infty f(\nu)\, d\nu \right] \quad (1)$$

where ν_0 is the center frequency of the symmetrical function $f(\nu)$. The second moments, so computed, are given in Table I.

For diamagnetic systems, Van Vleck[19] has shown that the second moment of powders can be calculated from the equation

$$\langle \Delta\nu^2 \rangle = {}^3/_5 g^4 \mu_N^4 \hbar^2 I(I+1) \sum_k r_{jk}^{-6} \quad (2)$$

where g is the nuclear g factor for a proton, μ_N is the nuclear magneton, h is Planck's constant, I is nuclear spin, and r_{jk} is the distance between nuclei j and k. Using eq 2, we have calculated the expected second moments, and these are given also in Table I. For the phenanthroline complexes we have no structural information so we have assumed standard C–C, C–N, and C–H bond distances and angles for a cis complex in the calculation. This result is essentially the second moment for one phenanthroline ligand since the second ligand contributes only 3% to the calculation due to the r^{-6} dependence. The order of magnitude difference between experiment and theory for the phenanthroline complexes cannot be accounted for by inaccuracies in the proton positions used in the calculation and must come from an intermolecular contribution from protons on neighboring complexes, which could not be included in the calculation.

The calculated second moments for the picolylamine complexes were done with use of reported crystal structure data[20-22] as a guide. Since no hydrogen positions are known, we had to assume reasonable C–H, N–H, and O–H bond distances and angles. The agreement between experiment and theory is more reasonable in these systems, and the differences could be attributed to inaccuracies in the assumed proton positions.

C. T_1 Measurements. T_1 for protons was measured from 120 K to room temperature for $Fe(phen)_2(NCS)_2$(ext). A plot of ln T_1 vs. T^{-1} is presented in Figure 6. Below the transition

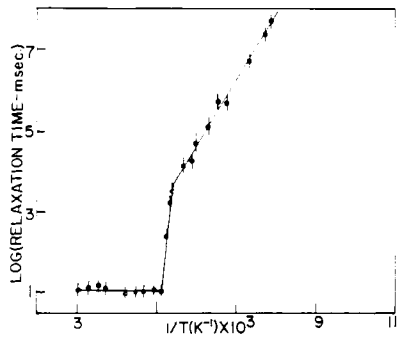

Figure 6. Plot of ln T_1 vs. reciprocal temperature for protons in $Fe(phen)_2(NCS)_2$ (ext).

temperature the data follow a straight line of slope 1.64×10^3 K and intercept −12.15. Above the transition temperature T_1 is a fixed value of 2.7 ms at all temperatures studied. An explanation for this behavior will be presented in the next section.

IV. Discussion

A. NMR Line Shape in the High-Spin State. The asymmetric line shape observed for $Fe(phen)_2(NCS)_2$(ext) in Figure 1 for the high-spin system can be quantitatively accounted for by using a dipolar model that has proven successful for rare-earth systems.[23,24] For a single proton at distance R from a metal ion, whose spin states are interconverting so rapidly that we can take an average over the spin states, the NMR paramagnetic shift is given by the equation[25]

$$\Delta\nu/\nu_0 = (\nu - \nu_0)/\nu_0 = (\chi/R^3)(3\cos^2\theta - 1) \quad (3)$$

where ν_0 is the resonance frequency in a diamagnetic system, χ is the paramagnetic susceptibility for one ion, and θ is the angle between the magnetic field and the **R** vector between the metal ion and the proton. This equation assumes that the unpaired electrons are only in d orbitals on the metal ion and that R is much greater than the average distance of the d electron from the metal ion so that a point-dipole approximation is valid. If the unpaired electron were to have some probability of being found in ligand atom orbitals, additional terms would have to be considered. These terms are here considered to be small compared to eq 3.

In a powder we have a statistical distribution of the possible values of θ and therefore a broad line. If no other broadening factors are present, the shape of the powder line is given by

$$g(\Delta\nu) = {}^1/_2[3A\nu_0(A\nu_0 + \Delta\nu)]^{-1/2} \qquad A = \chi/R^3 \quad (4)$$

where $\Delta\nu$ can take values only between $-A\nu_0$ and $+2A\nu_0$. If each crystallite gave a resonance with the shape function $h(\nu - \nu^\circ)$ where ν° is the center of the line, then the total powder pattern shape function, $I(\Delta\nu)$, would be given by

$$I(\Delta\nu) = \int g(y - \nu_0) h(\nu - y)\, dy \quad (5)$$

Putting eq 4 in (5) and defining

$$X^2 = A\nu_0 + y - \nu_0$$

we obtain

$$I(\Delta\nu) = (3a)^{-1/2} \int_0^{(3a)^{1/2}} h(\Delta\nu + a - x^2)\, dx \quad (6)$$

In our calculations we have assumed a Lorentzian shape function:

$$h(\Delta\nu) = T_2/[1 + (2\pi T_2)^2 \Delta\nu^2] \quad (7)$$

(19) Van Vleck, J. H. *Phys. Rev.* **1948**, *74*, 1168.
(20) Greenway, A. M.; Sinn, E. *J. Am. Chem. Soc.* **1978**, *100*, 8080.
(21) Greenway, A. M.; O'Connor, C. J.; Schroek, A.; Sinn, E. *Inorg. Chem.* **1979**, *18*, 2692.
(22) Katz, B. A.; Strouse, C. E. *J. Am. Chem. Soc.* **1979**, *101*, 6214.
(23) Mustafa, M. R.; McGarvey, B. R. *J. Magn. Reson.* **1977**, *25*, 341.
(24) Reuveni, A.; McGarvey, B. R. *J. Magn. Reson.* **1979**, *34*, 181.
(25) Kurland, R. J.; McGarvey, B. R. *J. Magn. Reson.* **1970**, *2*, 286.

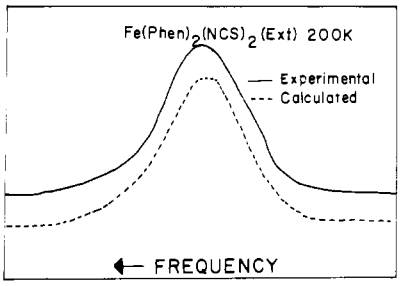

Figure 7. Comparison of the NMR resonance line shape of Fe(phen)$_2$(NCS)$_2$ (ext) at 200 K with a theoretical line shape calculated from a model described in the text.

We used eq 6 and 7 to calculate a resonance spectrum for each of the four different H atoms in the complex and then added up the four spectra to get our final result. χ was calculated from

$$\chi = \mu^2/3kT \tag{8}$$

with $\mu = 5.17\ \mu_B$.[3] The four metal–hydrogen distances were estimated to be 0.335, 0.524, 0.578, and 0.606 nm by assuming standard C–C, C–H, C–N, and N–Fe distances. We then varied the shortest value of R and the four line widths ($1/\pi T_2$) until we obtained our best fit, which is plotted in Figure 7 along with the experimental curve at 200 K. The best fit was obtained for $R = 0.360$ nm and line widths of 77.5, 76.5, 75.5, and 74.5 kHz.

Although the fit is not perfect and could probably be improved by assuming small contact shifts, which would change the center of each of the four lines, it is good enough to see that the model explains all the main features of the curves. The bump on the low-frequency side of the line is primarily due to the proton closest to Fe(II) and comes from those crystals in which the magnetic field is perpendicular to **R**. This is why adjustment of this R value is crucial to obtaining a good fit.

Since χ determines the shape and width of the paramagnetic resonances, the T^{-1} dependence of line width is expected and our experimental confirmation of this is a further confirmation of the above model. The model also predicts the observed frequency dependence of line width in the paramagnetic region.

B. Second Moments. The difference between the experimental and calculated second moments for Fe(phen)$_2$(NCS)$_2$(ext) must be due to an intermolecular contribution not included in the calculations. The magnitude of the intermolecular term is larger than that normally found in organic systems. This can best be appreciated by estimating how close the hydrogens on different phenanthroline molecules would have to be to give such a result. If we were to assume only one hydrogen on each molecule of phenanthroline came close to each other, the distance between them would be 0.173 nm to account for the observed intermolecular term. If two hydrogens on each phenanthroline ring were equally close, the distance would only be increased to 0.194 nm. These distances are similar to those H–H distances in CH_3 and CH_2 groups and would indicate that the hydrogens are close enough to produce some steric interference between hydrogen atoms on neighboring complexes.

It will be noted that a similarly large second moment is found for the Zn(II) analogue so that it is a general feature of the crystal structure and not peculiar to the Fe(II) complex alone. The larger second moment for Fe(phen)$_2$(NCS)$_2$(ppt) is due to the presence of ~12% paramagnetic Fe(II). The differences in the picolylamine complexes could be due to similar intermolecular effects, but in this case small changes in the assumed H–H distances in the CH_2^-, NH_2, and CH_3 groups present could result in removing much of the differences seen in Table I.

C. T_1 Measurements. The general features seen in the T_1 measurements on Fe(phen)$_2$(NCS)$_2$(ext) as shown in Figure 6 are the rapid decrease of T_1 with increasing temperature below the spin transition and the constancy of T_1 above that temperature. Consideration of these facts in terms of present theories of T_1 in paramagnetic systems reveals much useful information on the validity of present theories of the spin transition.

The theory of T_1 in diamagnetic systems having paramagnetic impurities was first presented by Bloembergen,[26] who postulated that the bulk magnetization relaxed by diffusion toward a paramagnetic site via the nuclear dipolar (or spin–spin flip) relaxation and then was equilibrated with the lattice by the interaction between the paramagnetic ion and nearby lattice nuclei. Two limiting cases were distinguished: diffusion-limited relaxation and rapid diffusion. In the first case the slow step is the rate of diffusion of the spin magnetization to the paramagnetic site. In the second case the rate is determined by the rate of equilibration of neighboring nuclei with the lattice via their interaction with the paramagnetic ion. Khutsishvili[27] and de Gennes[28] found equations for T_1 for the case of slow diffusion while Blumberg[29] obtained the equation for rapid diffusion. Rorschach[30] derived an equation for the region between the two limiting cases giving the earlier results as proper limits. All of these derivations assumed low concentrations of paramagnetic sites. Lowe and Tse[31] extended the theories to concentration regions where there can be more than one paramagnetic site. They found a new limiting case for very high concentrations of paramagnetic centers.

1. Lowe and Tse Limiting Cases. The appropriate limiting case is decided by the relative size of three parameters in the theory. They are as follows: (1) R, the radius of a sphere containing only one paramagnetic site; (2) b, the "barrier radius" inside of which spin diffusion is prevented because the local field of the paramagnetic ion has shifted the resonance of nuclei inside the barrier too far from the other nuclei so that the spin-flip mechanism (which requires both nuclei to have the same resonance frequency) is quenched; (3) $\beta = (\bar{C}/D)^{1/4}$ where D is the diffusion coefficient for spin diffusion and $\bar{C}$ is given by

$$\bar{C} = {}^2/_5\gamma_n{}^2\gamma_e{}^2\hbar^2 S(S+1)\tau_c \tag{9}$$

where τ_c is a correlation time for the z component of paramagnetic spin and the other symbols have their normal meaning. Lowe and Tse[31] distinguish the three limiting cases as

case 1: $R > b >> \beta$ (rapid diffusion)
case 2: $R >> \beta >> b$ (diffusion limited)
case 3: $\beta \geq R > b$ (diffusion vanishing)

For purposes of our later arguments we must establish that case 3 does not apply to our system because it has a different dependence on the concentration of paramagnetic sites from the other two.

We shall first estimate the three parameters for our sample when it is 100% paramagnetic. In this case $R \geq 0.7$ nm, which is the effective radius of the complex molecule itself. The value of b has been shown[32] to depend on crystal orientation, but since we are measuring an average from the center of a powder spectrum we would best take b to be the closest distance

(26) Bloembergen, N. *Physica (Amsterdam)* **1949**, *15*, 386.
(27) Khutsishvili, G. R. *Proc. Inst. Phys. Acad. Sci. Georgia (USSR)* **1956**, *4*, 3.
(28) de Gennes, P. G. *J. Phys. Chem. Solids* **1958**, *7*, 345.
(29) Blumberg, W. E. *Phys. Rev.* **1960**, *119*, 79.
(30) Rorschach, H. E., Jr. *Physica (Amsterdam)* **1964**, *30*, 38.
(31) Lowe, I. J.; Tse, D. *Phys. Rev.* **1968**, *166*, 279.
(32) Booth, R. J.; McGarvey, B. R. *Phys. Rev. B: Condens. Matter* **1979**, *21*, 1627.

between Fe(II) and a hydrogen atom or $b = 0.35$ nm. To get a value for β, we must estimate both τ_c and D. D we can estimate by using an equation given by Bloembergen:[26]

$$D = a^2/50T_2 \tag{10}$$

where a is the average distance between protons ($\sim$0.25 nm) and T_2 is determined from the second moment given in Table I. We find thus that $D \simeq 1.35 \times 10^{-16}$ m^2 s^{-1}, and taking $\tau_c = 10^{-12}$ s, we estimate that $\beta \simeq 0.26$ nm. This means that we have probably an intermediate case between cases 1 and 2 for the paramagnetic sample and for all lower concentrations of paramagnetic sites since R increases as concentration of paramagnetic sites decreases. The value of τ_c is a reasonable estimate and is confirmed by taking the limiting equations in both cases and calculating τ_c from the experimental value of T_1 in the 100% case. The calculations give τ_c values of 7.4 ps (case 1) and 4.6 ps (case 2). The same calculations give $\beta \sim b$, and this definitely puts us in the intermediate situation between case 1 and 2.

In both case 1 and 2 and the intermediate region considered by Rorschach,[30] T_1 is proportional to N^{-1} where N is the number of paramagnetic sites in a unit volume. The only temperature-dependent terms in the theory are N and τ_c. Above the spin-transition temperature N is constant, so that the invariance of T_1 in this region means that τ_c is constant from 188 to 300 K. If we can assume this constancy of τ_c holds to the lowest temperature studied, then we can use T_1 to measure the mole fraction of high-spin Fe(II), X, in the sample using the simple relationship

$$X = (T_1)_P/T_1 \tag{11}$$

where $(T_1)_P$ is the value of T_1 in system when $X = 1$. Equation 11 allows us to measure X in temperature regions unavailable to other techniques, and this in turn will allow us to check the predicted behavior of X vs. T in a low-concentration region where the theories take a simpler analytical form.

2. Zimmermann and König Theory (Ising-Type Theory). First we will compare our results with that predicted by the theory of Zimmermann and König.[16] We will develop their theory here in a simpler modified version that retains its essential features. They proposed that the free energy, G, of 1 mol of a high-spin–low-spin system could be written in the fashion

$$G = XG^\circ_H + (1 - X)G^\circ_L + I(X) + RT[X \ln X + (1 - X) \ln (1 - X)] \tag{12}$$

where G°_H and G°_L are respectively the free energies of pure high-spin (H) and low-spin (L) systems in the absence of any cooperative interaction terms, $I(X)$ is a cooperative interaction term, which is some function of the mole fraction of high spin, X, and the third term is an entropy of mixing term. In general we might expect $I(X)$ to have the form

$$I(X) = I_{LL}(1 - X)^2 + I_{LH}(1 - X)X + I_{HH}X^2 \tag{13}$$

where I_{LL} is the interaction term for a pair both having low spin, etc. For convenience this can be rewritten as

$$I(X) = J_0 + J_1X - J_2X^2 \tag{14}$$

The negative sign for J_2 is chosen to conform to that used by Zimmermann and König,[16] who only used the third term for $I(X)$ in their theory. At equilibrium $(\partial G/\partial X)_T = 0$, so that eq 12 and 14 will yield

$$X = [1 + e^{(\Delta G^\circ + J_1 - 2XJ_2)/RT}]^{-1} \tag{15}$$

This is the same equation obtained by Zimmermann and König[16] if we equate their J to our J_2 and their $\Delta - RT \ln \nu$ to our $\Delta G^\circ + J_1$. The critical temperature T_C has $X = {}^1/_2$ so that eq 15 gives

$$\Delta G^\circ + J_1 - J_2 = 0 = \Delta H^\circ - T_C\Delta S^\circ + J_1 - J_2 \tag{16}$$

or

$$T_C = (\Delta H^\circ + J_1 - J_2)/\Delta S^\circ$$

If we calculate (dX/dT) at T_C, we find that the slope becomes negative at

$$(J_2/RT_C) > 2$$

in which case we would get a discontinuous transition.

At low temperatures where X is small, eq 15 becomes

$$X \simeq e^{-(\Delta G^\circ + J_1)/RT} = e^{\Delta S^\circ/R}e^{-(\Delta H^\circ + J_1)/RT} \tag{17}$$

and $\ln T_1$ vs. T would follow the equation

$$\ln T_1 = \ln (T_1)_p - (\Delta S^\circ/R) + (\Delta H^\circ + J_1)/RT \tag{18}$$

This is the origin of the straight-line plot at low temperature seen in Figure 6. From the slope and intercept plus the value of $(T_1)_p$ we find

$$\Delta H^\circ + J_1 = 13.6 \pm 0.8 \text{ K J mol}^{-1} \quad \text{or} \quad 1139 \pm 7 \text{ cm}^{-1}$$

$$\Delta S^\circ = 51.8 \pm 0.9 \text{ J mol}^{-1} \text{ K}^{-1} \quad \text{or} \quad 0.433 \pm 0.008 \text{ cm}^{-1} \text{ K}^{-1}$$

This value of ΔS° agrees very well with the thermodynamic value of 48.78 ± 0.71 J mol^{-1} K^{-1} reported by Sorai and Seki.[9] Using eq 16 and $T_C = 188$ K, we find

$$J_2 = 3.85 \text{ kJ mol}^{-1} \quad \text{or} \quad 321.6 \text{ cm}^{-1}$$

It should be noted that $J_2/RT_C = 2.46$, which is greater than 2.0, which is in line with the observation of a discontinuous transition. Sorai and Seki[9] reported a value of 8.60 ± 0.14 kJ mol^{-1} for ΔH from their thermodynamic measurements. In this theory their ΔH would be equivalent to $\Delta H^\circ + J_1 - J_2$, which gives 9.8 kJ mol^{-1} for their ΔH.

The T_1 measurements are completely consistent with the Zimmermann–König[16] model and yield thermodynamic parameters that agree with thermodynamic measurements. In fact T_1 measurements are perhaps the easiest way to obtain these parameters.

3. Cluster Model. We must now consider how the T_1 results agree with predictions of the "cluster" model.[9,17,33] The theory of T_1 discussed above assumes a random distribution of paramagnetic ions rather than large clusters and must be revised to discuss the cluster model. For temperatures below the transition temperature, where we should be measuring T_1 only for the diamagnetic portion of the sample and not for any hydrogens inside the paramagnetic cluster, we can easily modify the present theories in the following manner. We assume that our paramagnetic sites are clusters of n ions rather than a single ion. The same theoretical equations should apply except that the following parameters are replaced by the effective values:

$$N_{eff} = N/n \qquad b_{eff} = n^{-1/3}b \qquad \bar{C}_{eff} = n^2\bar{C} \qquad \beta_{eff} = n^{-1/2}\beta \tag{19}$$

Since β_{eff} increases more than b_{eff}, we are now in the limited-diffusion region (case 2) where

$$T_1 = 3/(8\pi ND\beta) \tag{20}$$

which gives

$$T_1(\text{eff}) = n^{-1/2}T_1 \tag{21}$$

Thus we see that the T_1 we measure will still be proportional

(33) Hyde, J. S.; Rao, K. V. S. *J. Magn. Reson.* **1978**, *29*, 509.

to N^{-1} as before, but the mole fraction will now be given by the equation

$$X = n^{-1/2}(T_1)_p/T_1 \quad (22)$$

provided the limited-diffusion case is correct for the paramagnetic region also; otherwise we can only say X is proportional to T_1^{-1}. In the "cluster" theory X is given by

$$X = [1 + e^{n\Delta G^\circ/RT}]^{-1} \quad (23)$$

which becomes

$$X \simeq e^{n\Delta S^\circ/R}e^{-n\Delta H^\circ/RT} \quad (24)$$

for temperatures below the transition temperature where X is small. Thus a plot of ln T_1 vs. T^{-1} will again give a straight-line plot, but the slope will be $n(\Delta H^\circ/R)$. Using n = 95 found by Sorai and Seki,[9] we obtain ΔH° = 0.144 kJ mol^{-1}, which is very much different than the thermodynamic value of 8.60 ± 0.14 kJ mol^{-1}. With use of eq 22 the intercept of the straight-line plot would be

$$\ln (n^{-1/2}(T_1)_p) - n(\Delta S^\circ/R)$$

which gives ΔS° = 1.382 J K^{-1} mol^{-1}, which is again very much smaller than the value found from thermodynamic measurements. This would still be the case if eq 22 were modified to take into account the fact that $(T_1)_p$ is determined from the intermediate equations of Rorschach.[30]

What the above discrepancies are telling us is that the expected values of X from the cluster theory are orders of magnitude smaller in the low-temperature region than the values found by T_1 measurements. Thus the T_1 measurements do not support the "cluster" model at all.

V. Conclusions

NMR will prove a valuable tool in studying these solid-state spin transitions. In the case of $Fe(phen)_2(NCS)_2$ our studies show that the T_1 measurements are in drastic disagreement with the "cluster" model[9,17] but in complete agreement with the Zimmermann–König model.[16] This does not rule out the formation of clusters in the transition region itself, since they could play an important role in the kinetics of the transition. What is ruled out is the formation of stable large clusters at temperatures well below the transition temperature. We have also confirmed that the transition itself is kinetically slow (~30 min).

The second-moment results show the presence of close contact between hydrogen atoms on ligands attached to different iron ions. It is tempting to assume that this plays a role in the cooperative interaction between neighboring complexes. It could be, for example, that this close steric interaction prevents certain molecular vibrations in the complex from being independent of similar ones in adjacent molecules and the interaction energies result from destructive and constructive interferences in the vibronic energies of one molecule by the steric interaction with vibronic levels in an adjacent molecule.

We are puzzled as to what mechanism of fluctuation in the spin states of $^5T_2$ would give rise to a temperature independent τ_c, but the experimental results clearly show this to be the case in $Fe(phen)_2(NCS)_2$. We hope to study other Fe(II) spin-crossover systems to ascertain if this is generally the case. We also plan to study T_1 for the picolylamine systems, but a proper study will require modification of our probe to allow measurements well below 120 K, which is the practical limit at present.

Acknowledgment. This work was supported by the Natural Science and Engineering Research Council of Canada and by a NATO research grant (No. 1372).

Registry No. $Fe(phen)_2(NCS)_2$, 14692-67-2; $Zn(phen)_2(NCS)_2$, 15319-97-8; $Fe(pic)_3Cl_2$·EtOH, 62629-77-0; $Zn(pic)_3Cl_2$·EtOH, 78421-01-9; $Fe(pic)_3Cl_2$·MeOH, 62629-74-7; $Zn(pic)_3Cl_2$·MeOH, 78421-02-0.